ACS APPLIED MATERIALS & INTERFACES

Research Article

www.acsami.org

Graphene Nanoribbon/V_2O_5 Cathodes in Lithium-Ion Batteries

Yang Yang,[†,‡] Lei Li,[†] Huilong Fei,[†] Zhiwei Peng,[†] Gedeng Ruan,[†] and James M. Tour*[,†,‡,§]

[†]Department of Chemistry, [‡]Smalley Institute for Nanoscale Science and Technology, and [§]Department of Materials Science and NanoEngineering, Rice University, 6100 Main Street, Houston, Texas 77005, United States

Supporting Information

ABSTRACT: Nanocrystalline V_2O_5 particles were successfully entrapped by graphene nanoribbons (GNRs) derived from unzipped carbon nanotubes. The electrical conductivity of V_2O_5 nanoparticles was enhanced after introducing the GNRs. The 3-dimensional conductive framework in the composites plays a significant role in improving the rate performance and cyclability of the material when used as a cathode in lithium-ion batteries. By tailoring the mass ratio between the GNRs and the V_2O_5 nanoparticles, the fabricated composites can deliver a high capacity of 278 mAh g^{-1} at 0.1 *C*, which is close to its theoretical value, whereas a capacity of 165 mAh g^{-1} can be maintained at 2 *C*. The delivered capacity at 0.1 *C* can maintain 78% of its initial capacity after 100 cycles.

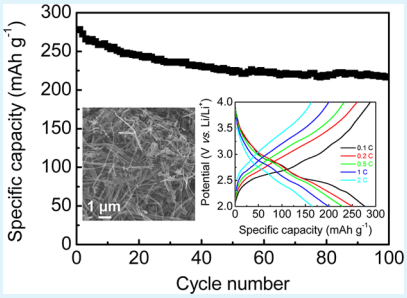

KEYWORDS: *graphene nanoribbons, V_2O_5, lithium ion batteries, cathode, cyclability*

INTRODUCTION

Graphene nanoribbons (GNRs) prepared by the longitudinal splitting of multiwalled carbon nanotubes (MWCNTs) are showing applications in a host of platforms.[1−5] Only recently, GNRs have been used as supporting materials for metal oxide composites in anodes for lithium-ion batteries (LIBs).[6] Compared to the conventionally used carbon additives such as carbon black and reduced graphene oxide (rGO), GNRs have advantages in forming composites with metal oxides. The nature of the interaction is not known, but the microscopy and performance substantiate the efficient interaction between the metal nanoparticles and the GNR surface presumably through efficient intercalation.[2] The result is nanoscale mixing, which should be superior to compositions made through mechanically mixing active materials with conductive additives such as carbon black.[1] Second, the active materials trapped in GNRs can buffer the volume expansion of the active materials during discharge, especially for composites with conversion and alloying charge storage mechanisms.[7] Recently, the edge effect in two-dimensional materials has been found to be crucial to their electrochemical performance.[8] On the basis of the unzipping mechanism,[1,2] a large number of edge sites are created during the formation of GNRs, which might produce more electrochemically active sites for charge transfer during charge/discharge when compared to rGO and carbon nanotubes. The formation of more edge sites in GNRs does not lead to a loss in the conductivity of the composites.[4] Before this report, the applications of GNRs in LIBs were focused on anodes and there has been no report on cathode composites using GNRs as the supporting materials.

V_2O_5 is one of the most investigated layered metal oxides for cathode materials in LIBs because of its high electrochemical activity, high energy density and much higher capacities than conventional cathode materials such as $LiCoO_2$ (140 mAh g^{-1}) and $LiFePO_4$ (170 mAh g^{-1}).[9−11] For V_2O_5, a theoretical capacity of 294 mAh g^{-1} is expected when discharged to 2 V (vs. Li/Li^+) which corresponds to two lithium intercalations. And an irreversible capacity of 440 mAh g^{-1} is anticipated from three lithium intercalations when discharged to 1.5 V (vs. Li/Li^+).[12] However, poor cyclability in V_2O_5 remains a problem for that cathode material due to degradation upon lithium diffusion and the poor conductivity of V_2O_5.[13] To address those problems, nanocrystalline V_2O_5 and conducting polymer coatings have been developed.[14,15] Based on our previous success in using GNRs to integrate with SnO_2 for high performance anodes,[8] in this work, we present an approach to entrap nanocrystalline V_2O_5 in the three-dimensional (3D) open framework of GNR arrays to minimize degradation or lithium diffusion and to improve the conductivity of the electrodes. The GNRs in the composites work not only as platforms to load V_2O_5 on their surfaces but also as a network that is conductive without any other carbon additives, such as carbon black, being needed. The as-prepared composite cathodes show enhanced LIB performance with improved cyclability by tailoring the mass ratio between the GNRs and V_2O_5.

RESULTS AND DISCUSSION

In this study, GNRs were prepared by Na/K-induced longitudinal splitting of MWCNTs (for the fabrication details, see Figure 1a and the Experimental Section).[2] Then V_2O_5 nanoparticles (NPs) were entrapped in the GNR composites by chemically intercalating VCl_4 with concomitant reduction by Na/K.[2] After postannealing at 250 °C for 3 h, V_2O_5 NPs can be

Received: April 1, 2014
Accepted: May 20, 2014
Published: May 20, 2014

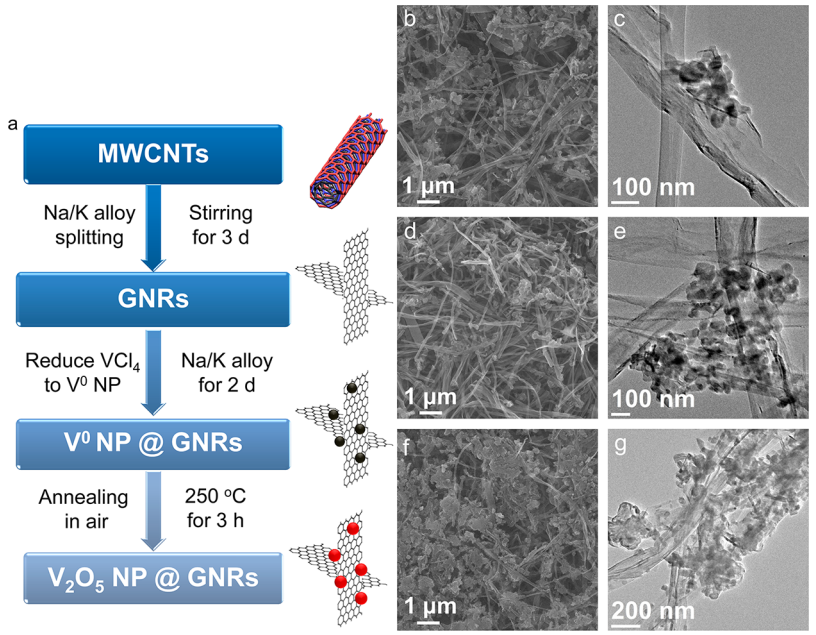

Figure 1. Synthesis scheme and microscopic images of the fabricated GNR-V_2O_5 NP composites. The composition of V_2O_5 entrapped in or on the GNRs could be tailored from 25, to 40, and 60 wt %, and these are designated as GNR25VO, GNR40VO and GNR60VO, respectively. (a) Schematic diagram of the fabrication process. (b) SEM and (c) TEM images of GNR25VO. (d) SEM and (e) TEM images of GNR40VO. (f) SEM and (g) TEM images of GNR60VO.

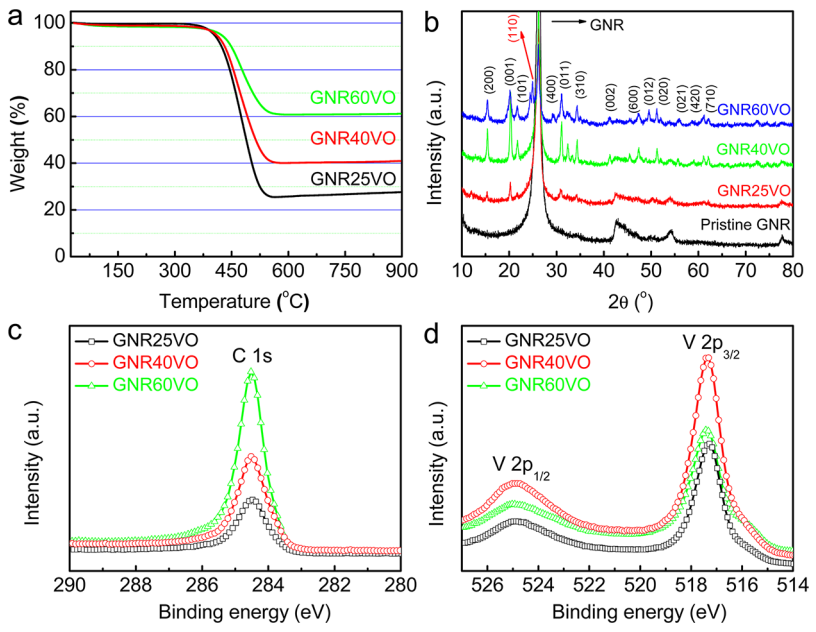

Figure 2. Investigations on the compositions and crystalline structures of the composites. (a) TGA analysis on the composites (in Ar, ramping rate 10 °C min^{-1}). (b) XRD of the composites. (c, d) XPS C 1s and V 2p spectra of the composites, respectively.

crystallized from the entrapped metallic vanadium. The amount of V_2O_5 NPs can be controlled by tailoring the amount of Na/K alloy used in the chemical intercalation process. The morphology changes due to the varied entrapping amounts of V_2O_5 NPs can be distinguished from SEM and TEM images (Figure 1b–g) of the post oxidized structures. It is clear that the amount of highly crystalline V_2O_5 NPs increase with increasing the Na/K alloy for the VCl_4 reduction. The average particle size of the final oxidized NPs ranges from 30–40 nm (see the Supporting Information, Figure S1). Although a higher entrapped amount of V_2O_5 NPs can be achieved by using more Na/K alloy relative to the amount of GNRs. As expected, the final oxidized V_2O_5 NPs are more easily aggregated at their higher weight fractions (Figure 1f, g) which might block the 3D open framework of the GNRs, thereby restricting lithium diffusion.

Further investigation on the composition and crystalline structure of the composites were performed by thermal gravimetric analysis (TGA, Figure 2a), X-ray diffraction (XRD, Figure 2b), and X-ray photoelectron spectroscopy (XPS, Figure 2c, d). Confirmed by TGA, the entrapped amounts of V_2O_5 NPs can be tailored from 25 to 40 and 60 wt

dx.doi.org/10.1021/am501969m | ACS Appl. Mater. Interfaces 2014, 6, 9590–9594

% by sequentially increasing the Na/K alloy content. A carbon peak (PDF #04−014−0362) at ∼26° indentified from XRD is ascribed to GNRs in the composites. Interestingly, the crystallinities of the composites with different amounts of V_2O_5 NPs are also different after postannealing. The diffraction peaks of V_2O_5 (Orthorhombic, PDF #00−041−1426) NPs have the lowest intensity for GNR25VO which indicates less crystalline material, whereas GNR40VO show a higher crystalline structure of V_2O_5. Though a crystalline structure can also be identified from GNR60VO, a diffraction peak at 24.9° (Monoclinic, PDF #04−003−4396) can be assigned to VO_2 (110),[16] which signifies that the metallic vanadium cannot be fully oxidized to V^{5+} at this higher loading of NP entrapment and negatively impacts its performance. Furthermore, the chemical compositions of the composites confirm the expected carbon at 284.5 eV, vanadium at 517.1 eV and oxygen at 530.1 eV by XPS (Figure 2c, d and the Supporting Information), Figure S2. The binding energy of vanadium and oxygen as determined in XPS indicates the formation of V-oxides in the composites.[17]

The cyclic voltammograms (CVs) show the positions of redox peaks for the reversible redox reactions between the different valence states of vanadium. To avoid irreversible formation of ω-phase $Li_xV_2O_5$ ($x > 2$), a potential window range from 2 to 4 V (vs. Li/Li^+) was applied at a scan rate of 0.5 mV s^{-1}. Three pairs of redox peaks at 2.7, 3.0, and 3.3 V in anodic sweep, 3.2 (R1), 2.8 (R2), and 2.4 V (R3) in cathodic sweep distinguished from CVs (Figure 3a, b) can be assigned to the different stages during lithium reversibly intercalating into V_2O_5 according to $V_2O_5 + xLi^+ + xe^- \leftrightarrows Li_xV_2O_5$.[18] More specifically, the R3, R2, and R1 reduction peaks are recognized as the continuous formation of different lithiated-V_2O_5 phases, i.e., ε-$Li_xV_2O_5$ ($0.35 < x < 0.7$), δ-$Li_xV_2O_5$ ($x = 1$), and γ-$Li_xV_2O_5$ ($1 < x < 3$), respectively.[9,18] There is an expected larger hysteresis (increased from ∼0.2 V in GNR25VO and GNR40VO to ∼0.5 V in GNR60VO) and lessened reversibility from the CVs of GNR60VO due to its relatively poor conductivity (Figure 3a and the Supporting Information, Figure S3). Galvanostatic discharge/charge (Figure 3c) was performed on the composites at 0.1 *C* to investigate their LIB performances. The quasi-platforms distinguished in discharge curves at 3.2, 2.9, 2.5 V and in charge curves at 2.6, 2.9, and 3.2 V indicate different stages of lithium intercalation/deintercalation as confirmed by the CVs. More promising is that GNR40VO delivers a discharge capacity of 278 mAh g^{-1}, which is close to the theoretical capacity of V_2O_5 for two lithium intercalations (294 mAh g^{-1}). However, the composite with lower crystallinity, GNR25VO, has a lower capacity of 208 mAh g^{-1}. It is known that cathode material with higher crystallinity can deliver better electrochemical performance.[18] With GNR60VO, a capacity of 185 mAh g^{-1} is obtained together with a large *iR* drop because of its higher inner resistance.

Different current densities from 0.1 to 2 *C* were applied on the composites to investigate their rate performances (Figure 4a). For GNR25VO, a capacity of 75 mAh g^{-1} is obtained at 2 *C*, whereas an improved rate capacity of 165 mAh g^{-1} is obtained from GNR40VO at 2 *C*. However, further increasing the amount of V_2O_5 NPs to 60 wt % results in a rapidly decayed capacity to <10 mAh g^{-1} at 2 *C* because of the lower conductivity and lower V_2O_5 crystallinity of that composite. From the discharge/charge curves of GNR40VO measured at different *C*-rates (Figure 4b), the quasi-platforms are still clear

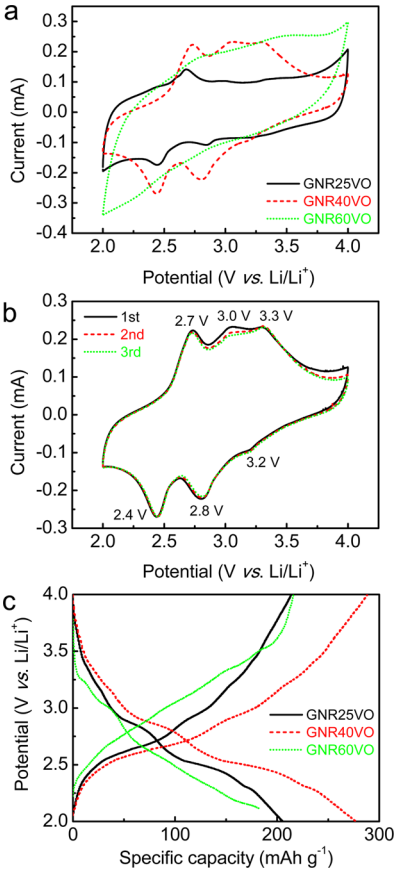

Figure 3. Electrochemical lithium intercalation/deintercalation performance of the composites. (a) CVs of the composites performed over a potential window from 2 to 4 V at a scan rate from 0.5 mV s^{-1}. (b) Initial three CVs cycles of the GNR40VO. (c) Discharge/charge profiles of the composites obtained at a current density of 0.1 *C*.

even at 2 C indicating fast kinetics for lithium intercalation/deintercalation. Moreover, cyclability is the most challenging aspect for practical LIB applications when using V_2O_5 as a cathode material. While being tested at 0.1 *C* for 100 cycles, GNR40VO delivers a greatly improved stability, > 78% capacity retention, compared with GNR25VO and GNR60VO (Figure 4c). The facilitated lithium intercalation kinetics resulting from the 3-D GNR networks and well-dispersed V_2O_5 NPs affect improved cyclability for GNR40VO. The improved conductivity can be demonstrated in the electrochemical impedance spectra (EIS, Figure 4d). It is clear that the charge transfer resistance (R_{ct}) for GNR40VO is reduced to 110 Ω, whereas a lower conductivity is found in GNR60VO with R_{ct} of 280 Ω. With lower V_2O_5 content, GNR25VO has a R_{ct} of 190 Ω. Thus, there is an optimal loading of V_2O_5 in the GNR composite to promote proper conductivity, crystallinity and accessibility for lithium ion migration. Thus, the as-fabricated GNR-V_2O_5 NP composites show improved rate performance and cyclability.[19−21]

CONCLUSION

In summary, a composite fabricated by entrapping 40 wt % V_2O_5 NPs on GNRs delivers a high capacity of 278 mAh g^{-1} at 0.1 C and 165 mAh g^{-1} at 2 *C* as well as a capacity retention >78% after 100 cycles of testing at 0.1 *C*. Enhanced conductivity contributed from the GNR frameworks and the stability of the V_2O_5 NPs endowed by the composite material

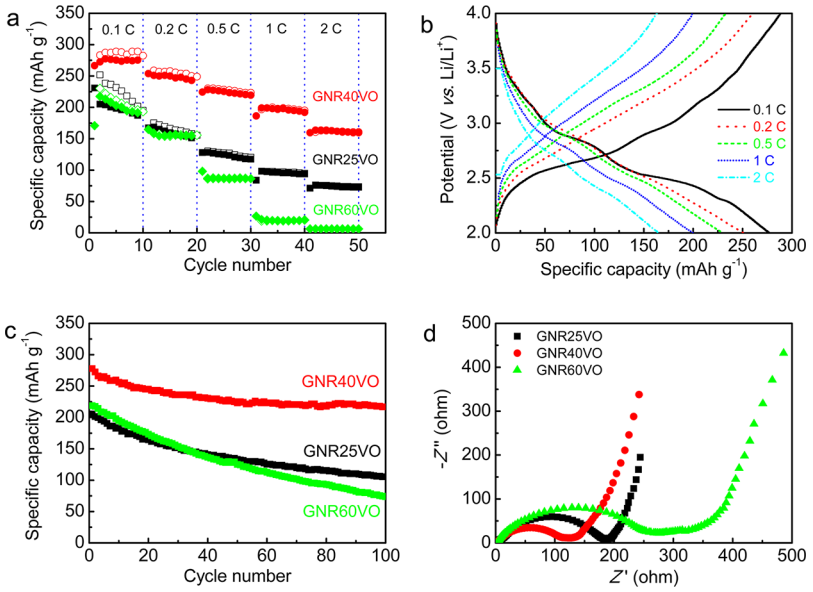

Figure 4. Rate performance and cyclability of the composites. (a) Variation in the capacity of the composites with different applied current densities from 0.1 to 2 *C*. (b) Discharge/charge profiles of the GNR40VO at different current densities from 0.1 to 2 *C*. (c) 100 discharge/charge cycle testing of the composites at 0.1 *C*. (d) EIS of the composites.

permits fast kinetics for lithium intercalation/deintercalation in LIB cathodes.

EXPERIMENTAL SECTION

Fabrication of GNRs from Unzipped MWCNTs. The synthesis of GNRs was achieved by unzipping MWCNTs (Mitsui Chemicals, for the experimental details see ref 2). Fifty milligrams of MWCNTs were added to an oven-dried 250 mL round-bottom flask, which was transferred to a glovebox under a N_2 atmosphere. Then 20 mL of freshly distilled 1,2-dimethoxyethane and 0.15 mL Na/K alloy were added into the flask to mix with MWCNTs and form a suspension. ***Caution**: All synthetic steps involving Na/K alloy should be carried out with extreme caution under strict exclusion of air or moisture and under inert gas and appropriate personal protection (hood, blast shields, face shield, and protective and fire resistant clothing) should be used and worn at all times.* Before taking the flask out of the glovebox, careful sealing of the flask with a septum was done. At room temperature, the suspension in the sealed flask was vigorously stirred for 3 days. Afterward, the suspension was quenched by adding 10 mL of methanol and the solution was stirred for another 10 min. Then the product was filtered through a 0.45 μm pore size PTFE membrane and washed sequentially with 100 mL of THF, 100 mL of i-PrOH, 100 mL of H_2O, 100 mL of i-PrOH, 100 mL of THF, and 100 mL of Et_2O. The final GNRs were then dried under vacuum (pressure 1×10^2 Torr) at room temperature for 24 h.

Fabrication of GNRs-V_2O_5 NPs Composites. Fifty milligrams of GNRs were mixed with 20 mL of freshly distilled 1,2-dimethoxyethane and different amounts, i.e., 0.1, 0.2, or 0.3 mL, of Na/K alloy in an oven-dried 250 mL round-bottom flask under N_2 atmosphere in glovebox. VCl_4 (liquid, Sigma-Aldrich, molar ratio VCl_4:Na/K = 4:1) was then added to the mixture solution with vigorous stirring for 2 d at room temperature. In this process, V^{4+} was reduced to V^0 NPs by the Na/K alloy while intercalating into the GNRs stacks. The mixture was then quenched with methanol and washed sequentially with THF, i-PrOH and H_2O followed by filtering over a 0.45 μm pore size PTFE membrane. The composites were dried under vacuum (pressure 1×10^2 Torr) at 60 °C for 24 h, and annealed at 250 °C (ramping speed 10 °C min^{-1}) in air for 3 h to oxidize the metallic vanadium to vanadium oxides without the loss of GNRs that would occur at higher temperatures.

ASSOCIATED CONTENT

Supporting Information

Experimental details and supplementary figures. This material is available free of charge via the Internet at http://pubs.acs.org.

AUTHOR INFORMATION

Corresponding Author

*E-mail: tour@rice.edu.

Notes

The authors declare no competing financial interest.

ACKNOWLEDGMENTS

We thank the Peter M. and Ruth L. Nicholas Post-Doctoral Fellowship of the Smalley Institute for Nanoscale Science and Technology for financial support (Y.Y.). Additional funding was provided by the ONR MURI Program (00006766, N00014-09-1-1066), AFOSR MURI program (FA9550-12-1-0035) and the AFOSR (FA9550-09-1-0581).

REFERENCES

(1) Kosynkin, D. V.; Higginbotham, A. L.; Sinitskii, A.; Lomeda, J. R.; Dimiev, A.; Price, B. K.; Tour, J. M. Longitudinal Unzipping of Carbon Nanotubes to Form Graphene Nanoribbons. *Nature* **2009**, *458*, 872−876.

(2) Genorio, B.; Lu, W.; Dimiev, A. M.; Zhu, Y.; Raji, A. -R. O.; Novosel, B.; Alemany, L. B.; Tour, J. M. *In Situ* Intercalation Replacement and Selective Functionalization of Graphene Nanoribbon Stacks. *ACS Nano* **2012**, *6*, 4231−4240.

(3) Shimizu, T.; Haruyama, J.; Marcano, D. C.; Kosinkin, D. V.; Tour, J. M.; Hirose, K.; Suenaga, K. Large Intrinsic Energy Bandgaps in Annealed Nanotube-Derived Graphene Nanoribbons. *Nat. Nanotechnol.* **2011**, *6*, 45−50.

(4) Kosynkin, D. V.; Lu, W.; Sinitskii, A.; Pera, G.; Sun, Z.; Tour, J. M. Highly Conductive Graphene Nanoribbons by Longitudinal Splitting of Carbon Nanotubes Using Potassium Vapor. *ACS Nano* **2011**, *5*, 968−874.

(5) Rafiee, M. A.; Lu, W.; Thomas, A. V.; Zandiatashbar, A.; Rafiee, J.; Tour, J. M.; Koratkar, N. A. Graphene Nanoribbon Composites. *ACS Nano* **2010**, *4*, 7415−7420.

(6) Lin, J.; Peng, Z.; Xiang, C.; Ruan, G.; Yan, Z.; Natelson, D.; Tour, J. M. Graphene Nanoribbon and Nanostructured SnO_2 Composite Anodes for Lithium Ion Batteries. *ACS Nano* **2013**, *7*, 6001−6006.
(7) Yan, M.; Wang, F.; Han, C.; Ma, X.; Xu, X.; An, Q.; Xu, L.; Niu, C.; Zhao, Y.; Tian, X.; Hu, P.; Wu, H.; Mai, L. Nanowire Templated Semihollow Bicontinuous Graphene Scrolls: Designed Construction, Mechanism, and Enhanced Energy Storage Performance. *J. Am. Chem. Soc.* **2013**, *135*, 18176−18182.
(8) Voiry, D.; Yamaguchi, H.; Li, J.; Silva, R.; Alves, D. C. B.; Fujita, T.; Chen, M.; Asefa, T.; Shenoy, V. B.; Eda, G.; Chhowalla, M. Enhanced Catalytic Activity in Strained Chemically Exfoliated WS_2 Nanosheets for Hydrogen Evolution. *Nat. Mater.* **2013**, *12*, 850−855.
(9) Yang, Y.; Albu, S. P.; Kim, D.; Schmuki, P. Enabling the Anodic Growth of Highly Ordered V_2O_5 Nanoporous/Nanotubular Structures. *Angew. Chem., Int. Ed.* **2011**, *50*, 9071−9075.
(10) Cao, A.-M.; Hu, J.-S.; Liang, H.-P.; Wan, L.-J. Self-Assembled Vanadium Pentoxide (V_2O_5) Hollow Microspheres from Nanorods and Their Application in Lithium-Ion Batteries. *Angew. Chem., Int. Ed.* **2005**, *44*, 4391−4395.
(11) Liu, J.; Xia, H.; Xue, D.; Lu, L. Double-Shelled Nanocapsules of V_2O_5-Based Composites as High-Performance Anode and Cathode Materials for Li Ion Batteries. *J. Am. Chem. Soc.* **2009**, *131*, 12086−12087.
(12) Sato, Y.; Nomura, T.; Tanaka, H.; Kobayakawa, K. Charge-Discharge Characteristics of Electrolytically Prepared V_2O_5 as a Cathode Active Material of Lithium Secondary Battery. *J. Electrochem. Soc.* **1991**, *138*, L37−L39.
(13) Wang, Y.; Zhang, H. J.; Siah, K. W.; Wong, C. C.; Lin, J.; Borgna, A. One Pot Synthesis of Self-Assembled V_2O_5 Nanobelt Membrane *via* Capsule-Like Hydrated Precursor as Improved Cathode for Li-Ion Battery. *J. Mater. Chem.* **2011**, *21*, 10336−10341.
(14) Sides, C. R.; Martin, C. R. Nanostructured Electrodes and the Low-Temperature Performance of Li-Ion Batteries. *Adv. Mater.* **2005**, *17*, 125−128.
(15) Wong, H. P.; Dave, B. C.; Leroux, F.; Harreld, J.; Dunn, B.; Nazar, L. F. Synthesis and Characterization of Polypyrrole/Vanadium Pentoxide Nanocomposite Aerogels. *J. Mater. Chem.* **1998**, *8*, 1019−1027.
(16) Guiton, B. S.; Gu, Q.; Prieto, A. L.; Gudiksen, M. S.; Park, H. Single-Crystalline Vanadium Dioxide Nanowires with Rectangular Cross Sections. *J. Am. Chem. Soc.* **2005**, *127*, 498−499.
(17) Mendialdua, J.; Casanova, R.; Barbaux, Y. XPS studies of V_2O_5, V_6O_{13}, VO_2 and V_2O_3. *J. Electron Spectrosc. Relat. Phenom.* **1995**, *71*, 249−261.
(18) Xu, H. Y.; Wang, H.; Song, Z. Q.; Wang, Y. W.; Yan, H.; Yoshimura, M. Novel Chemical Method for Synthesis of LiV_3O_8 Nanorods as Cathode Materials for Lithium Ion Batteries. *Electrochim. Acta* **2004**, *49*, 349−353.
(19) Chou, S. L.; Wang, J. Z.; Sun, J. Z.; Wexler, D.; Forsyth, M.; Liu, H. K.; MacFarlane, D. R.; Dou, S. X. High Capacity, Safety, and Enhanced Cyclability of Lithium Metal Battery Using a V_2O_5 Nanomaterial Cathode and Room Temperature Ionic Liquid Electrolyte. *Chem. Mater.* **2008**, *20*, 7044−7051.
(20) Noerochim, L.; Wang, J. Z.; Wexler, D.; Rahman, M. M.; Chen, J.; Liu, H. K. Impact of Mechanical Bending on The Electrochemical Performance of Bendable Lithium Batteries with Paper-Like Free-Standing V_2O_5-Polypyrrole Cathodes. *J. Mater. Chem.* **2012**, *22*, 11159−11165.
(21) Rui, X.; Zhu, J.; Sim, D.; Xu, C.; Zeng, Y.; Hng, H. H.; Lim, T. M.; Yan, Q. Reduced Graphene Oxide Supported Highly Porous V_2O_5 Spheres as a High-Power Cathode Material for Lithium Ion Batteries. *Nanoscale* **2011**, *3*, 4752−4758.